Self-assembly of retinoid nanoparticles for melanoma therapy

*Han Liao, Shan Zhao, Huihui Wang, Yang Liu, Ying Zhang, Guangwei Sun**

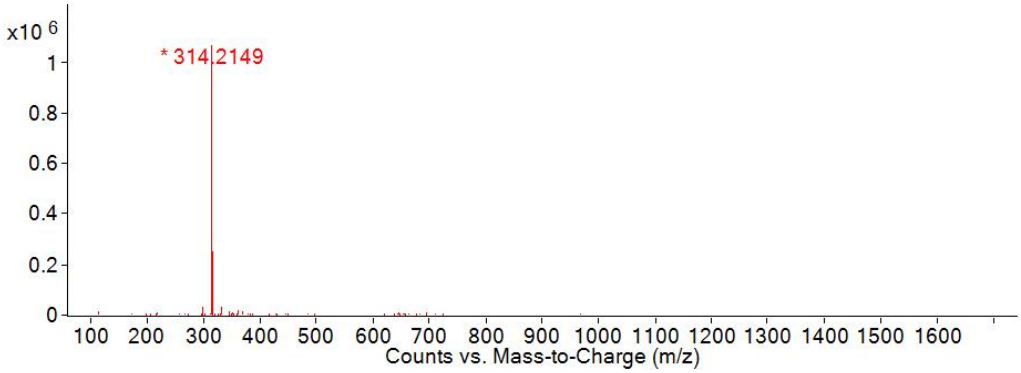

Fig. S1 ESI-mass spectrum of RHA. Negative ionization mode was used.

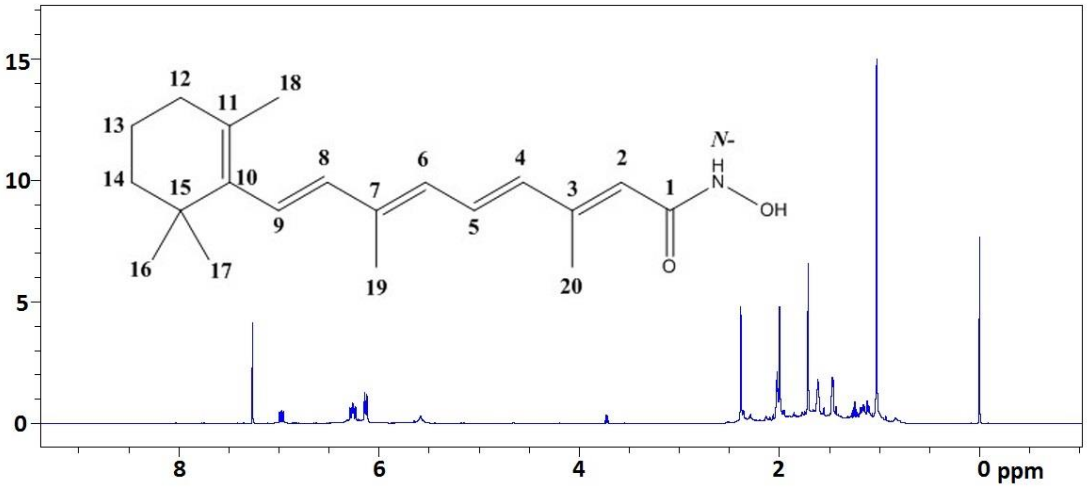

Fig. S2 ^{1}H-NMR spectrum of RHA using $CDCl_3$ as a solvent. Details were listed in table S1 below

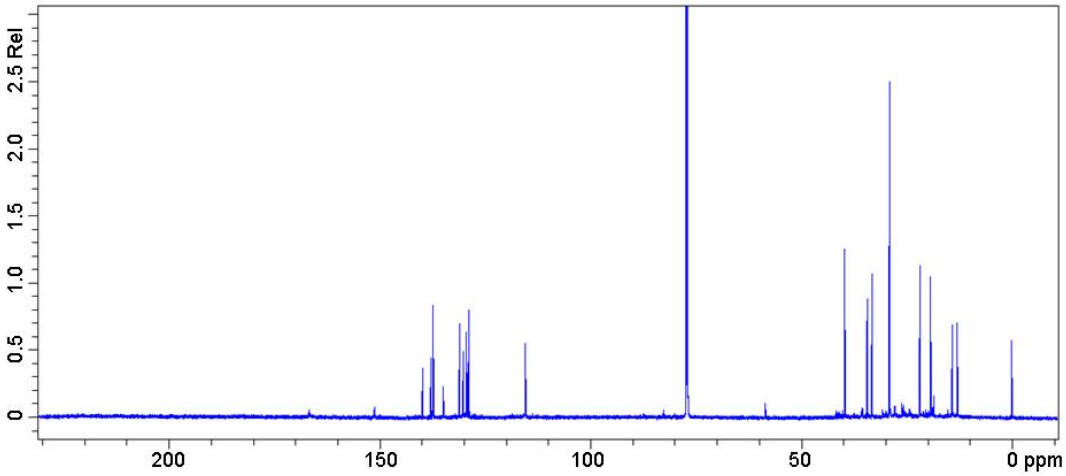

Fig. S3 ^{13}CNMR spectrum of RHA. $CDCl_3$ was used as solvent. Details were listed in table S2 below

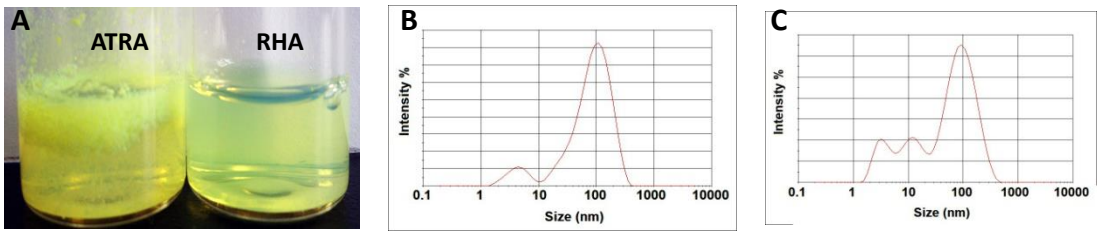

Fig. S4 (A) Appearance of ATRA and RHA nanoparticles 10 min after preparation and size distribution of (B) RHA NPs in fetal bovine serum. Pure fetal bovine serum (C) was used as background control.

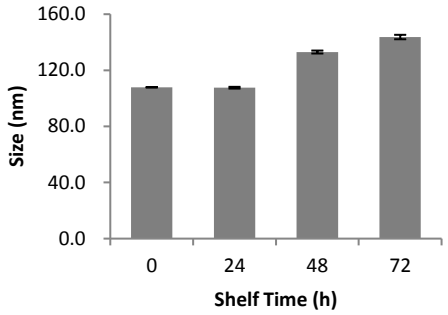

Fig. S5 Size of RHA nanoparticles after stored at room temperature for various time

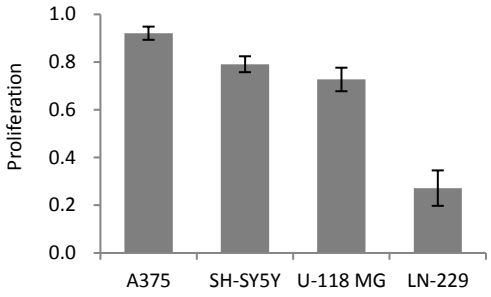

Fig. S6 Proliferation of various cell lines treated with 100 μM ATRA for 48 h (n=4).

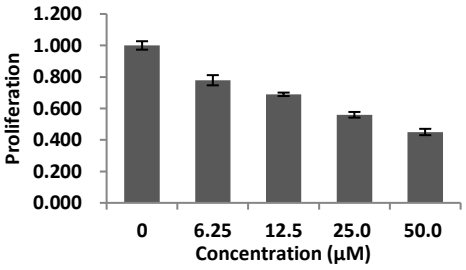

Fig. S7 Proliferation of L929 mouse fibroblast cells treated with RHA for 48 h (n=4).

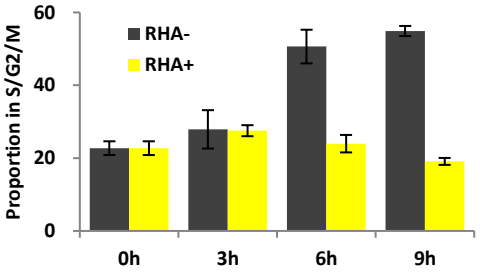

Fig. S8 DNA content analysis of late G1 synchronized A375 cells

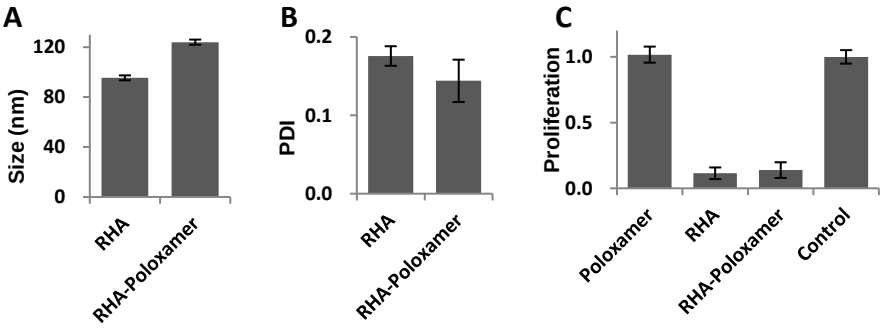

Fig. S9 Size(A), PDI(B), and Cytotoxicity(C) of RHA and RHA-Poloxamer nanoparticles (n=3)

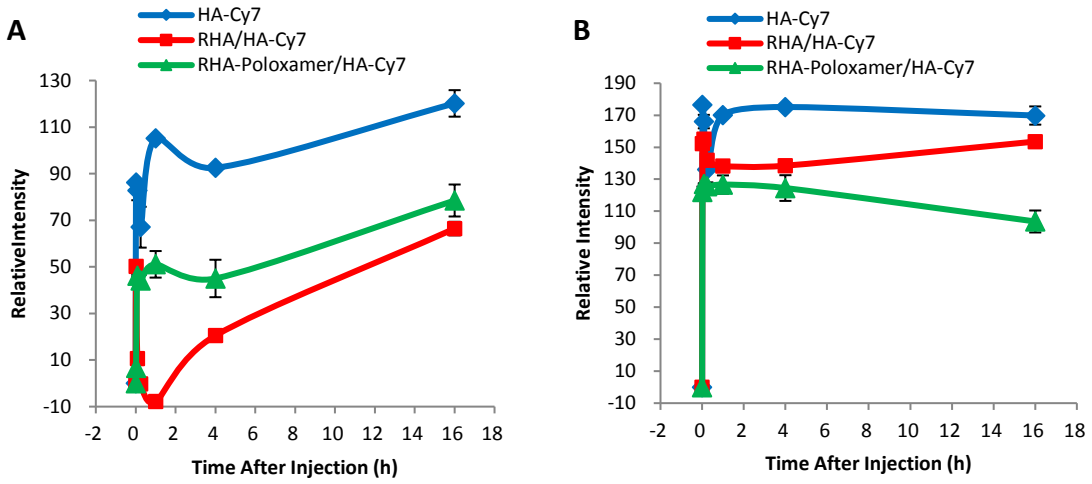

Fig. S10 Relative fluorescent intensity of tumor(A) and liver (B). Values were quantified using imageJ

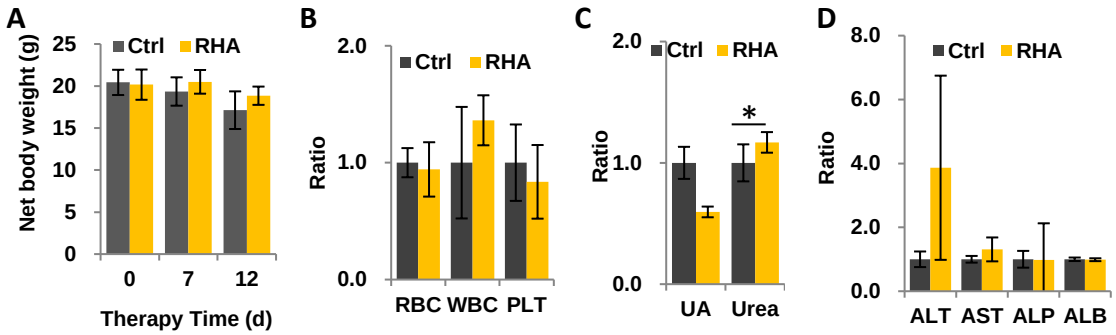

Fig. S11 Net body weight (A), Blood routine (B), kidney function related serum biochemistry (C), and liver function related serum biochemistry indexes (D) of mice. RHA therapy began at the 14th day of tumor bearing. Data were shown as mean with SD error bars (n=3). Significance difference: * ($P < 0.05$). Abbreviations: albumin (ALB), alkaline phosphatase (ALP), alanine aminotransferase (ALT), aspartate aminotransferase (AST), platelet (PLT), red blood cells (RBC), write blood cells (WBC), and uric acid (UA).

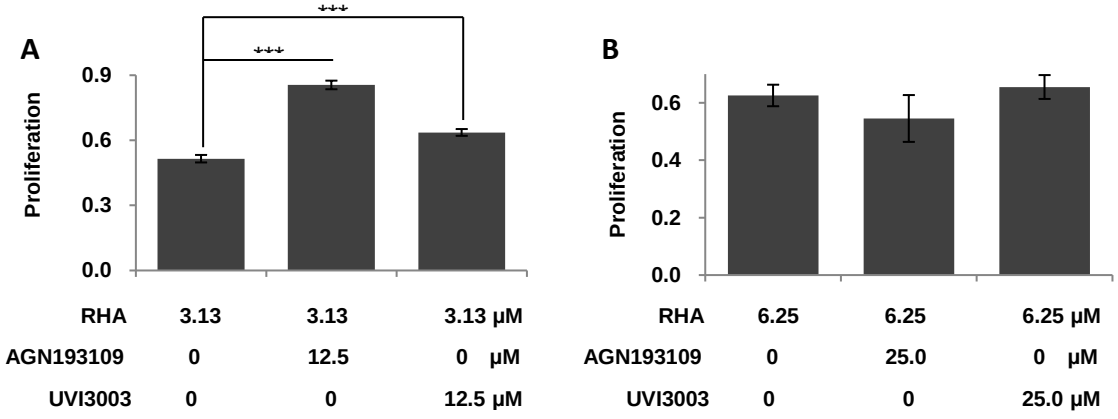

Fig. S12 Effect of RAR antagonist (AGN193109) and RXR antagonist (UVI3003) on anticancer activity of RHA (n=3). A: HL-60 cells, B: A375 cells. Significance difference: *** ($P < 0.001$)

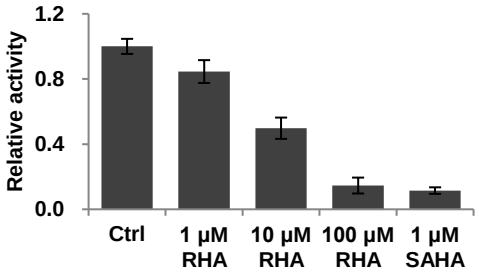

Fig. S13 Histone deacetylase inhibition activity of RHA. Vorinostat (SAHA) was used as positive control (n=3).

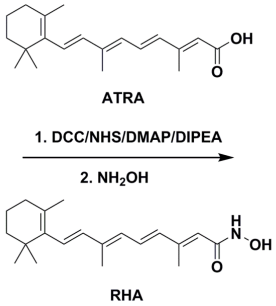

Scheme S1 Illustration of the RHA synthetic route achieved via a one-pot activated ester methodology.

Table S1 Details of ^{1}HNMR spectrum of RHA

Site	Chemical Shift (ppm)	Integral	Peaks	J (Hz)
N-	7.2630	1.000	s	/
2	5.5836	1.108	s	/
4, 6	6.2597	1.951	dd	23.491, 15.649
5	6.9735	0.849	dd	14.914, 11.553
8, 9	6.1319	1.980	d+dd	8.2620, 8.2620
12	2.0214	2.333	t	5.7064
13	1.6166	2.616	m	5.7414
14	1.4692	2.302	t	5.7064
16, 17	1.0276	6.228	s	/
18	1.7111	3.373	s	/
19	1.9872	3.268	s	/
20	2.3757	6.228	s	/

Table S2 Details of ^{13}CNMR spectrum of RHA

Site	Chemical Shift (ppm)	Site	Chemical Shift (ppm)
1	166.6111	11	130.0483
2	115.3219	12	33.1104
3	151.1109	13	19.2162
4	134.7989	14	39.5955
5	128.7710	15	34.2693
6	130.9425	16	28.9925
7	137.2207	17	28.9600
8	137.6997	18	21.7539
9	129.3364	19	14.0350
10	139.7076	20	12.9241